D-GLDPC Codes with 3-D Single Parity-Check Product Codes as Super Check Nodes

Yejun He*, Guiyuan Sun*†, Jie Yang*†, and Francis C. M. Lau†‡
* College of Information Engineering, Shenzhen University, 518060, China
† Department of Electronic and Information Engineering, The Hong Kong Polytechnic University, China
‡ Shenzhen Research Institute, The Hong Kong Polytechnic University, China

Email: {heyejun, sunguiyuan66, yangjie8925}@126.com, encmlau@polyu.edu.hk

***Abstract*—A doubly-generalized low-density parity-check (D-GLDPC) code is a low-density parity-check (LDPC) code, where both of the check nodes and variable nodes use linear block codes instead of repetition and single parity-check (SPC) codes. In this paper, we propose a class of D-GLDPC codes in which 3-dimensional (3-D) single parity-check product-codes (SPC-PCs) are used as super-check nodes (SCNs). We derive the extrinsic information transfer (EXIT) function of 3-D SPC-PCs used as SCNs, and analyze the performance of the proposed D-GLDPC codes over the additive white Gaussian noise (AWGN) channel with EXIT charts. Numerical analysis from EXIT charts shows that our proposed D-GLDPC codes can offer better decoding threshold than D-GLDPC codes with 2-D SPC-PCs as SCNs.**

Keywords*—3-D SPC-PC; D-GLDPC; EXIT chart; decoding threshold.

I. Introduction

Researchers have always been trying to find achievable coding schemes that have a low complexity and a threshold performance close to the Shannon limit. Low-density parity-check (LDPC) code, which was originally introduced by Gallager in 1960s [1] and resurrected in 1990s [2], is such a practical good code. Tanner also made significant contributions to the development of LDPC code in [3]. On the one hand, he vividly depicted the encoding and decoding characteristics of LDPC code by using the bipartite graph (also called Tanner graph). On the other hand, he introduced generalized LDPC (GLDPC) code.

The main idea of constructing a GLDPC code is to replace the single parity-check (SPC) code, which is used as the check node of an LDPC code, by short linear block code with powerful error-correcting capability. This approach improves the overall code performance by increasing the number of parity-check equations in the check nodes. Based on the above theory, Hamming codes, BCH codes, RS codes, RM codes and Hadamard codes have been used as (super-)check nodes [4-7].

In low code rate coding strategy, GLDPC codes provide a good solution to obtain a good trade-off between waterfall performance and error floor, but they increase the decoding complexity resulted from introducing more complex linear block code. Such (super-)check nodes need to apply more powerful a-posteriori-probability (APP) decoder. Furthermore, the overall code rate is reduced [8]. The rate loss problem can be solved if the repetition code constraints at the variable nodes are also generalized to linear block code with higher code-rate. This code was known as doubly-generalized LDPC (D-GLDPC) code, which was firstly introduced in [9]. The generalized variable nodes and check nodes without using repetition codes or SPC codes are called super-variable nodes (SVNs) and super-check nodes (SCNs), respectively. Those block codes, whose minimum distances meet the constraint $d_{min} \geqslant 2$ at SVNs or SCNs, are referred to as the component codes (subcodes) of the D-GLDPC code. In particular, they are named as generalized variable or check component codes. The set of all SVNs and SCNs are also regarded as variable-node decoders (VNDs) and check-node decoders (CNDs), respectively.

Analysis of the stability condition over the binary erasure channel (BEC) suggests that three attractive features (high code rate, minimum distance of 2 and easy to decode) make SPC code an attractive candidate to be the variable component code [10], [11]. In [12] and [13], a class of D-GLDPC codes, using 2-D SPC-PCs as SCNs and SPC codes as SVNs, with good performance and low complexity are investigated over an additive white Gaussian noise (AWGN) channel and binary phase-shift keying (BPSK) modulation. In this paper, we elaborate on this idea and extend 2-D SPC-PCs to 3-D SPC-PCs, while SPC codes are still used as SVNs.

The remainder of this paper is organized as follows. In Section II, the D-GLDPC code and the SPC-PC are reviewed. Our proposed D-GLDPC codes are described in Section III. More precisely, the EXIT curves of 3-D SPC-PCs used as SCNs are firstly derived. Then, EXIT charts of the proposed D-GLDPC codes are plotted, and finally the decoding threshold and convergence behavior of the proposed D-GLDPC codes are analyzed. Concluding remarks and future work are given in Section IV.

II. Preliminaries

A. Overview of a D-GLDPC code

Similar to an LDPC code, a D-GLDPC code with length N and dimension K can be represented by a Tanner graph, where nodes can also be divided into two disjoint parts, namely SVNs and SCNs. There are no connections among SVNs, neither do SCNs. Fig. 1 depicts the Tanner graph of a D-GLDPC code with N_a SVNs and M_a SCNs. These nodes are defined by

978-1-4799-7339-2/14/$31.00 ©2014 IEEE

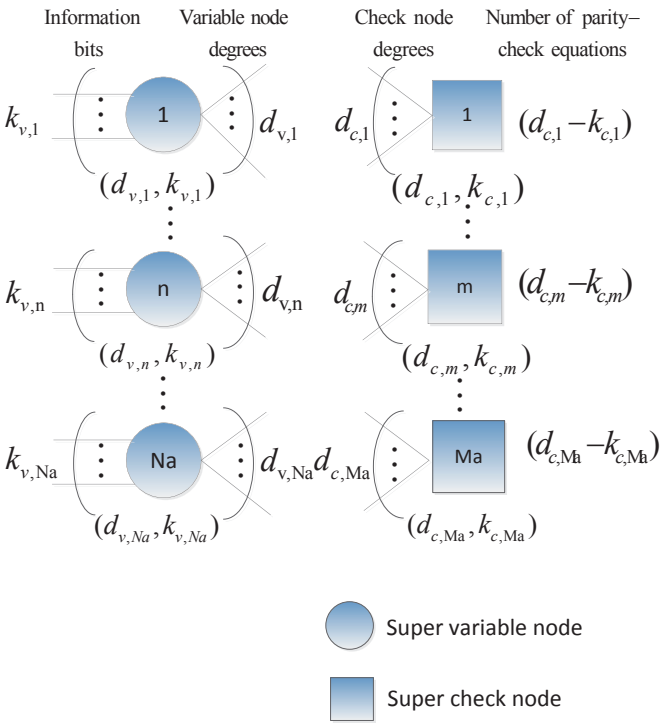

Fig. 1. Graph representation of a D-GLDPC code.

a sparse binary $M_a \times N_a$ matrix, denoted by $\mathbf{H}_a$, which is named as the adjacency matrix. If the (m,n)-th entry $H_{m,n}$ in $\mathbf{H}_a$ is equal to "1", it indicates that the m-th SCN has a connection with the n-th SVN.

The n-th SVN, denoted by $(d_{v,n}, k_{v,n})$, receives $k_{v,n}$ information bits from the communication channel and encodes them into $d_{v,n}$ local code bits, i.e., the SVN is connected by $d_{v,n}$ edges in the graph. Hence $d_{v,n}$ is the degree of this SVN and is equal to the weight of n-th column of $\mathbf{H}_a$. When $k_{v,n} = 1$, a SVN becomes a repetition variable node in an LDPC code.

The m-th SCN, denoted by $(d_{c,m}, k_{c,m})$, is connected with $d_{c,m}$ edges of the graph and contains $(d_{c,m} - k_{c,m})$ parity-check equations. $d_{c,m}$ is also the degree of this SCN and is equal to the weight of m-th row of $\mathbf{H}_a$. A SPC check node is simply a particular case where $(d_{c,m} - k_{c,m}) = 1$.

The overall length of a D-GLDPC code is given by

$$N = \sum_{n=1}^{N_a} k_{v,n} \tag{1}$$

Considering that redundant check equations may exist, the total number of valid check bits M of a D-GLDPC code has an upper bound given by

$$M \leq \sum_{m=1}^{M_a} (d_{c,m} - k_{c,m}) \tag{2}$$

Therefore, the code-rate of a D-GLDPC code is lower-bounded by

$$R \geq 1 - \sum_{n=1}^{M_a} (d_{c,m} - k_{c,m}) / \sum_{n=1}^{N_a} k_{v,n} \tag{3}$$

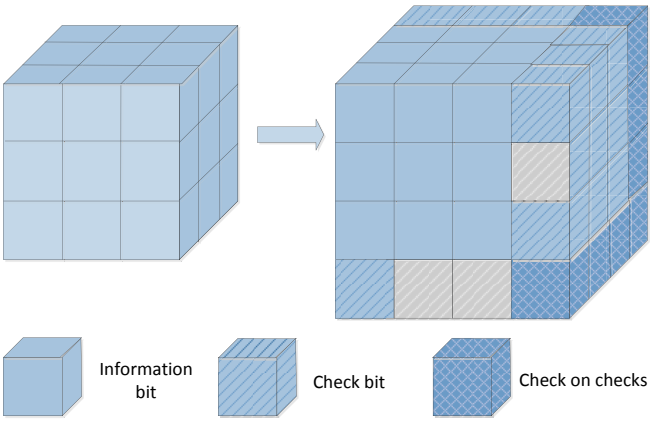

Fig. 2. Structure of $(4,3)^3$ SPC-PC.

D-GLDPC codes also have regular and irregular forms. A D-GLDPC code is said to be regular if all of its SVNs are of the same type and all the SCNs are of the same type. Otherwise, it is said to be irregular. Especially, the D-GLDPC is strongly regular if all SVNs use the same generator matrix. In general, irregular D-GLDPC codes have better performance than regular ones. For simplicity, we only consider regular D-GLDPC codes in this work. Moreover, all the SPC codes used as SVNs are in systematic form.

B. Single parity-check product codes (SPC-PCs)

Product codes, introduced by Elias in 1954, are serially concatenated codes. In this section, a special type of product codes, which is constructed by binary and systematic SPC codes, called SPC-PC is introduced. SPC-PC [14], denoted by $(n, n-1)^d$, means each SPC component code has a code length n and dimension $(n-1)$ in each of the d dimensions. Each dimension has n^{d-1} SPC codes. Hence the block length of the resultant d-dimensional product code is

$$N_{SPC-PC} = n \times n^{d-1} = n^d \tag{4}$$

and the number of information bits is

$$K_{SPC-PC} = (n-1)^d. \tag{5}$$

The code rate is therefore equal to

$$R_{SPC-PC} = K_{SPC-PC}/N_{SPC-PC} = [(n-1)/n]^d. \tag{6}$$

When $d_1 > d_2$, the code rate of d_1-dimensional SPC-PC is lower than d_2-dimensional SPC-PC with the same overall code length or component code length. For example, for the same overall code length of 64, the rate of the 3-D $(4,3)$ SPC-PC is given by $R_{(4,3)^3} = 27/64$ and is smaller than that of the 2-D $(8,7)$ SPC-PC which has a rate of $R_{(8,7)^2} = 49/64$; the 3-D $(4,3)$ SPC-PC has a lower code rate than the 2-D $(4,3)$ SPC-

PC. It implies that SPC-PCs with a higher dimension generally have a better error correction performance than those with a lower dimension under the same channel parameter E_b/N_0.

A 3-D $(n, n-1)$ SPC-PC can be viewed as n 2-D $(n, n-1)$ SPC-PC stacked on top of one another. Furthermore, each column in the stack is governed by the same $(n, n-1)$ SPC component code. In Fig. 2, we illustrate the structure of a $(4,3)^3$ SPC-PC. The code can be viewed as four $(4,3)^2$ SPC-PC stacked on top of one another, forming a $4 \times 4 \times 4$ cube. Moreover, the information bits of size $3 \times 3 \times 3$ are arranged in the upper left corner of the cube while the parity-check bits are located on bottom, right and back surfaces of the cube. The code has an overall length of $n^3 = 4^3 = 64$ and $(n-1)^3 = 3^3 = 27$ information bits. Thus, total number of valid check bits equals $M_{SPC-PC} = n^3 - (n-1)^3 = (3n^2 - 3n + 1) = 64 - 27 = 37$ and the code rate is $R_{SPC-PC} = (3/4)^3 = 27/64$.

In a 3-D SPC-PC, each dimension contains n^2 SPC component codes and each SPC code corresponds to one parity-check equation. Thus, the total number of parity-check equations equals

$$\tilde{M}_{SPC-PC} = 3n^2. \tag{7}$$

Note that the total number of parity-check equations above $(3n^2)$ is larger than the number of valid check bits $(3n^2 - 3n+1)$ and hence some parity-check equations are redundant. In the following, we describe the redundancy based on the corresponding parity-check matrix.

The corresponding parity-check matrix (denoted by $\mathbf{H}_{SPC-PC}$) of a 3-D $(n, n-1)$ SPC-PC has a size of $\tilde{M}_{SPC-PC} \times N_{SPC-PC} = 3n^2 \times n^3$ and can be expressed as

$$\mathbf{H}_{SPC-PC} = \begin{bmatrix} \mathbf{A} \\ \mathbf{B} \\ \mathbf{C} \end{bmatrix}_{3n^2 \times n^3} \tag{8}$$

$$\mathbf{A} = \begin{bmatrix} \mathbf{e}_n^{\mathrm{T}} & \mathbf{0} & \mathbf{0} & \cdots & \mathbf{0} & \mathbf{0} \\ \mathbf{0} & \mathbf{e}_n^{\mathrm{T}} & \mathbf{0} & \cdots & \mathbf{0} & \mathbf{0} \\ \mathbf{0} & \mathbf{0} & \mathbf{e}_n^{\mathrm{T}} & \cdots & \mathbf{0} & \mathbf{0} \\ \vdots & \vdots & \vdots & \ddots & \vdots & \vdots \\ \mathbf{0} & \mathbf{0} & \mathbf{0} & \cdots & \mathbf{e}_n^{\mathrm{T}} & \mathbf{0} \\ \mathbf{0} & \mathbf{0} & \mathbf{0} & \cdots & \mathbf{0} & \mathbf{e}_n^{\mathrm{T}} \end{bmatrix}_{n^2 \times n^3} \tag{9}$$

$$\mathbf{B} = \begin{bmatrix} \mathbf{B_1} & \mathbf{0} & \mathbf{0} & \cdots & \mathbf{0} & \mathbf{0} \\ \mathbf{0} & \mathbf{B_1} & \mathbf{0} & \cdots & \mathbf{0} & \mathbf{0} \\ \mathbf{0} & \mathbf{0} & \mathbf{B_1} & \cdots & \mathbf{0} & \mathbf{0} \\ \vdots & \vdots & \vdots & \ddots & \vdots & \vdots \\ \mathbf{0} & \mathbf{0} & \mathbf{0} & \cdots & \mathbf{B_1} & \mathbf{0} \\ \mathbf{0} & \mathbf{0} & \mathbf{0} & \cdots & \mathbf{0} & \mathbf{B_1} \end{bmatrix}_{n^2 \times n^3} \tag{10}$$

$$\mathbf{B_1} = \begin{bmatrix} \mathbf{I}_n & \mathbf{I}_n & \cdots & \mathbf{I}_n \end{bmatrix}_{n \times n^2} \tag{11}$$

$$\mathbf{C} = \begin{bmatrix} \mathbf{I}_{n^2} & \mathbf{I}_{n^2} & \cdots & \mathbf{I}_{n^2} \end{bmatrix}_{n^2 \times n^3} \tag{12}$$

where $\mathbf{e}_n^{\mathrm{T}}$ is all-one vector of size $1 \times n$, $\mathbf{0}$ is a vector/matrix of appropriate size, $\mathbf{I}_n$ and $\mathbf{I}_{n^2}$ are the $n \times n$ and $n^2 \times n^2$ identity matrix, respectively.

$\mathbf{H}_{SPC-PC}$ can be divided into three row blocks each of size $n^2 \times n^3$. Rows $1 \sim n^2$ correspond to parity-check equations of the first dimension and do not contain any redundancy; Rows $(n^2+1) \sim 2n^2$ correspond to the second dimension with rows $n^2+n, n^2+2n, \ldots, n^2+n^2$ (total n rows) being redundant; Rows $(2n^2+1) \sim 3n^2$ correspond to the third dimension with Rows $2n^2+n, 2n^2+2n, \ldots, 2n^2+(n-2)n, 2n^2+(n-1)n, 2n^2+(n-1)n+1, 2n^2+(n-1)n+2, \ldots, 2n^2+(n-1)n+n$ (total $2n-1$ rows) being redundant. These redundant rows correspond to the checks on checks and there are $(3n-1)$ such rows in total.

The error or erasure correction capability of a code generally improves with its minimum distance. In [14], it has been pointed out that the minimum Hamming distance of the $(n, n-1)^d$ SPC-PC is equal to

$$d_{min} = 2^d. \tag{13}$$

That is to say, the minimum distance is growing exponentially with the number of dimensions, which makes the 3-D SPC-PC more robust to errors, thereby offering better error-correcting performance comparing with 2-D SPC-PC.

C. EXIT chart analysis

Using density evolution to analyze the theoretical performance of a D-GLDPC code is very difficult. Fortunately, EXIT charts can be applied [9]. The EXIT chart is an effective tool to visualize and analyze the convergence behavior of decoders by tracking the evolution of the mutual information [15]. The EXIT chart includes two EXIT curves: one represents the EXIT function of the SVNs and the other represents that of the SCNs. Each curve is plotted according to the relationship between the average *a priori information* $(I_{a,svn}/I_{a,scn})$ and the average extrinsic information $(I_{e,svn}/I_{e,scn})$ of the constituent decoder. It is worth noting that in an EXIT chart, the EXIT curve of the variable-node decoder (VND) plots $I_{e,svn}$ against $I_{a,svn}$ for a given communication channel parameter, while the EXIT curve of the check-node decoder (CND) plots $I_{a,scn}$ against $I_{e,scn}$.

For a D-GLDPC code, the closed-form EXIT functions of SVN and SCN over the binary erasure channel (BEC) under maximum a posteriori (MAP) decoding have been derived in [10]. For general (n_{svn}, k_{svn}) SVNs and (n_{scn}, k_{scn}) SCNs, the closed-form EXIT functions can be written as

$$\begin{aligned} I_{e,svn}^{BEC}(p,q) = 1 - \frac{1}{n_{svn}} \sum_{t=0}^{n_{svn}-1} \sum_{z=0}^{k_{svn}} p^t (1-p)^{n_{svn}-t-1} \\ q^z (1-q)^{k_{svn}-z} \times [(n_{svn}-t)\tilde{e}_{n_{svn}-t,k_{svn}-z} \\ -(t+1)\tilde{e}_{n_{svn}-t-1,k_{svn}-z}] \end{aligned} \tag{14}$$

$$\begin{aligned} I_{e,scn}^{BEC}(p) = 1 - \frac{1}{n_{scn}} \sum_{t=0}^{n_{scn}-1} p^t (1-p)^{n_{scn}-t-1} \\ \times [(n_{scn}-t)\tilde{e}_{n_{scn}-t} - (t+1)\tilde{e}_{n_{scn}-t-1} \end{aligned} \tag{15}$$

where q and p are the erasure probabilities of the communi-

cation channel and the extrinsic channel of BEC, respectively. The (g,h)-th split information function, denoted by $\tilde{e}_{g,h}$, is defined as the summation of the ranks of all the possible sub-matrices obtained by choosing g columns in the corresponding generator matrix with the size of $k_{svn} \times n_{svn}$ and h columns in the corresponding $k_{svn} \times k_{svn}$ identity matrix. $\tilde{e}_g$ is the g-th un-normalized information function and is defined as the summation of the ranks of all the possible sub-matrices obtained by selecting g columns in the corresponding generator matrix $k_{scn} \times n_{scn}$. It is noted that $\tilde{e}_g$ is independent of the representations of SCN. Namely, different generator matrix expressions of the same SCN lead to the same EXIT function, which greatly simplifies the calculation of information function.

III. Proposed D-GLDPC codes and Analyses

Our proposed D-GLDPC codes use the same type of SPC codes at SVNs and the same type of 3-D SPC-PCs at SCNs. The proposed D-GLDPC code is therefore regular. Moreover, all the SPC codes are in systematic form. The SPC code is one of the most popular error detection codes because it is easy to implement. When it is introduced as the component code at the SVN in a D-GLDPC, its high code rate can compensate the overall code rate loss of the original GLDPC.

A. EXIT curves for 3-D SPC-PC used as SCNs

The generator matrix of a 3-D SPC-PC has no uniform form and so it is not easy to get its EXIT function directly. Fortunately, the special form of its parity-check matrix $\mathbf{H}_{SPC-PC}$ given in (7) is also the generator matrix of its dual code [16]. Suppose we can obtain the information function $\tilde{e}_g$ of its dual code. Then we make use of the following equations

$$I_e^{\perp}(p) = 1 - I_e(1-p) \quad (16)$$

$$I_{a,scn} = 1 - p \quad (17)$$

where $I_e^{\perp}(p)$ represents the EXIT function of the dual code to obtain the EXIT function of a 3-D SPC-PC which is used as SCN. Using (15), the EXIT function of the dual code of the 3-D SPC-PC used as SCN is therefore given by

$$I_{e,scn}^{\perp}(p) = 1 - \frac{1}{n^3}\sum_{t=0}^{n^3-1} p^t(1-p)^{n^3-1-t} \times[(n^3-t)\tilde{e}_{n^3-t} - (t+1)\tilde{e}_{n^3-t-1}] \quad (18)$$

where $\tilde{e}_g$ is found by summing the ranks of all the possible sub-matrices obtained by choosing g columns from the generator matrix of this dual code, which is also the parity-check matrix of the 3-D SPC-PC $\mathbf{H}_{SPC-PC}$. It can be readily shown that the information function $\tilde{e}_g$ can be approximately given by

$$\tilde{e}_g \approx \begin{cases} g \cdot C_{n^3}^g, & g < (3n^2-3n+1) \\ (3n^2-3n+1)\cdot C_{n^3}^g, & g \geq (3n^2-3n+1) \end{cases} \quad (19)$$

which is used in our following analyses.

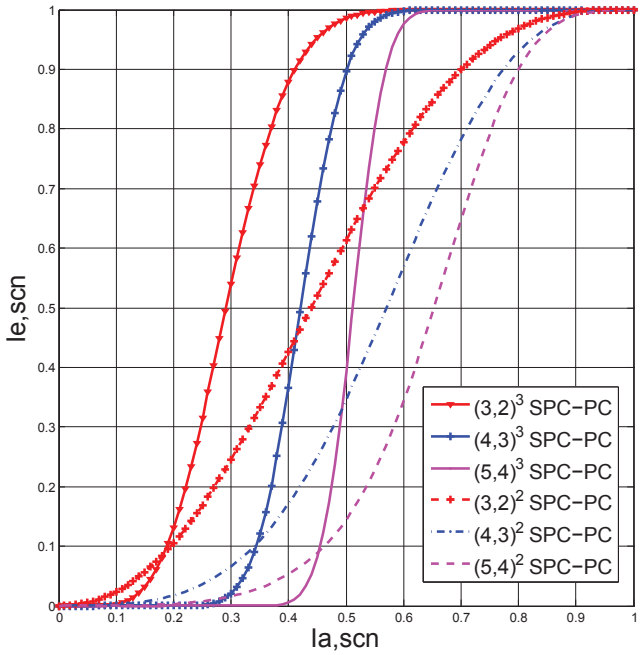

Fig. 3. EXIT curves for 3-D and 2-D SPC-PCs used as SCNs.

Based on the above, the EXIT function of the 3-D SPC-PC is expressed as

$$\begin{aligned} I_{e,scn}^{BEC}(p) &= 1 - I_{e,scn}^{\perp}(1-p) \\ &= \frac{1}{n^3}\sum_{t=0}^{n^3-1}(1-p)^t p^{n^3-1-t} \\ &\quad \times[(n^3-t)\tilde{e}_{n^3-t} - (t+1)\tilde{e}_{n^3-t-1}]. \end{aligned} \quad (20)$$

Hence,

$$\begin{aligned} I_{e,scn}^{BEC}(I_{a,scn}) &= \frac{1}{n^3}\sum_{t=0}^{n^3-1}(I_{a,scn})^t(1-I_{a,scn})^{n^3-1-t} \\ &\quad \times[(n^3-t)\tilde{e}_{n^3-t} - (t+1)\tilde{e}_{n^3-t-1}]. \end{aligned} \quad (21)$$

The EXIT curves for different 3-D and 2-D SPC-PCs used as SCNs are illustrated in Fig. 3 by exploting (21). We can observe that above a certain threshold $l'_{a,scn}$ and for the same SPC component code, the EXIT curve of 3-D SPC-PC outperforms that of 2-D SPC-PC in terms of extrinsic information.

B. EXIT charts of proposed D-GLDPC codes

When 3-D $(n, n-1)$ SPC-PCs are used as the SCNs and SPCs of length N_{spc} are used as SVNs in our proposed regular D-GLDPC codes, the code rate R is given by

$$\begin{aligned} R &= 1 - \frac{M_a \times M_{SPC-PC}}{N_a \times (N_{spc}-1)} \\ &= 1 - \frac{M_a \times (3n^2-3n+1)}{N_a \times (N_{spc}-1)} \end{aligned}$$

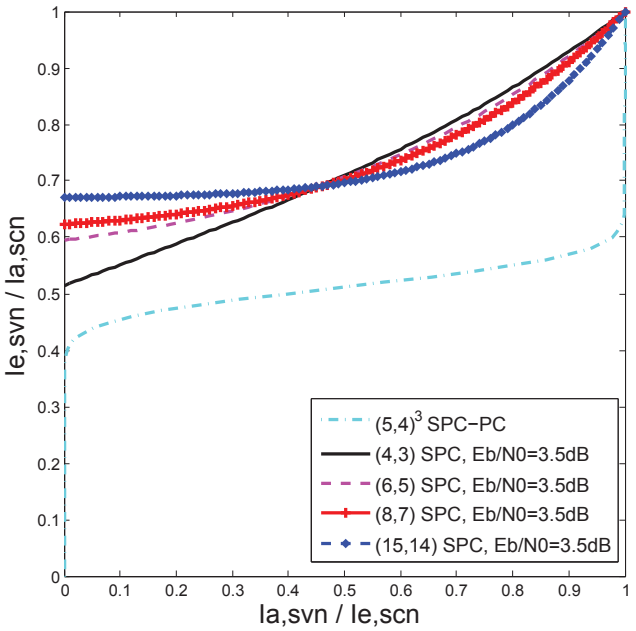

Fig. 4. EXIT charts of D-GLDPC codes with $(5,4)^3$ SPC-PCs as SCNs and different SPC codes as SVNs over the AWGN channel at $E_b/N_0 = 3.5$ dB. The overall code rates corresponding to SVN using $(15,14), (8,7), (6,5)$ and $(4,3)$ SPC are $0.477, 0.442, 0.414$ and 0.349, respectively.

$$= \quad 1 - \frac{N_{spc} \times (3n^2 - 3n + 1)}{n^3 \times (N_{spc} - 1)}. \tag{22}$$

For an AWGN channel with the channel parameter E_b/N_0 (in dB), an EXIT curve of a SVN can be estimated by making the substitution [17]

$$q = 1 - J(\sqrt{8 \times R \times 10^{\frac{E_b/N_0}{10}}}) \tag{23}$$

where $J(\cdot)$ is given in the Appendix of [15].

Assuming that 3-D $(5,4)$ SPC-PCs are used at the SCNs, we plot $I_{a,scn}$ against $I_{e,scn}$ in Fig. 4. Assuming an AWGN channel with a parameter $E_b/N_0 = 3.5$ dB, we evaluate the code rate of the overall D-GLDPC code and q using (22) and (23), respectively, when different SPCs are used at the SVNs. The overall code rates corresponding to SVN using $(15,14), (8,7), (6,5)$ and $(4,3)$ SPC are $0.477, 0.442, 0.414$ and 0.349, respectively. Subsequently, we plot the EXIT curves of these SPCs in Fig. 4 by substituting (23) and $I_{a,svn} = 1-p$ into (14) and by using the exact split information function for SPC codes found in [18]. It can be seen there is a large gap (or tunnel) between the EXIT curve of each SPC code and that of the SPC-PC. The result implies that the mutual information is expected to converge to the point (1,1) on the chart and hence the codeword can be decoded successfully under such conditions.

Fig. 5 plots the EXIT chart of a D-GLDPC code with $(5,4)^3$ SPC-PCs as SCNs and $(8,7)$ SPC codes as SVNs when the channel parameter E_b/N_0 varies. The overall code rate is $R = 0.442$. As channel parameter E_b/N_0 decreases, the tunnel between the VND curve and CND curve becomes narrower.

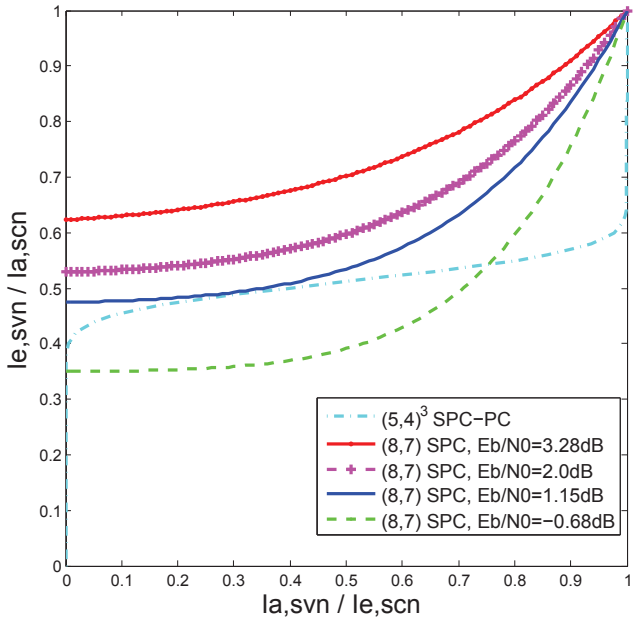

Fig. 5. EXIT chart of a D-GLDPC code with $(8,7)$ SPC codes as SVNs and $(5,4)^3$ SPC-PCs as SCNs at different E_b/N_0. The overall code rate is 0.442.

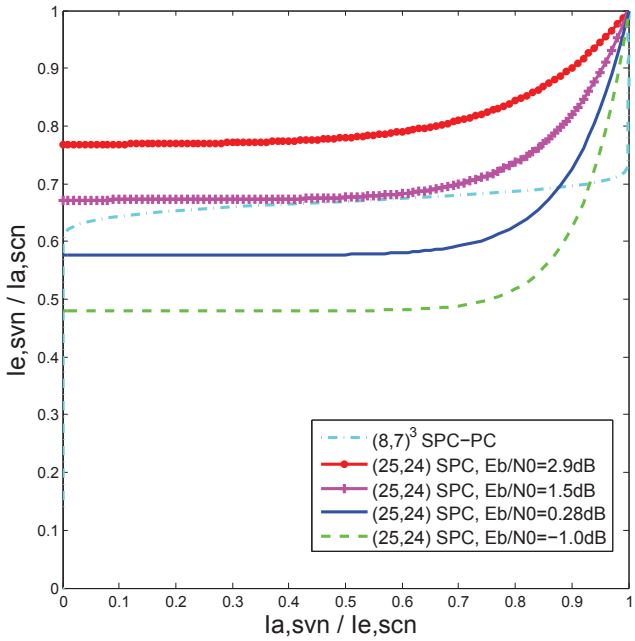

Fig. 6. EXIT chart of a D-GLDPC code with $(25,24)$ SPC codes as SVNs and $(8,7)^3$ SPC-PCs as SCNs at different E_b/N_0. The overall code rate is 0.656.

At $E_b/N_0 = 1.15$ dB, the two curves touch at another point in addition to (1,1). It implies that the mutual information is not expected to converge to the point (1,1) and hence the decoding will fail. Thus, the decoding threshold of this D-GLDPC code is $E_b/N_0 = 1.15$ dB.

Fig. 6 shows the EXIT chart of a D-GLDPC code with

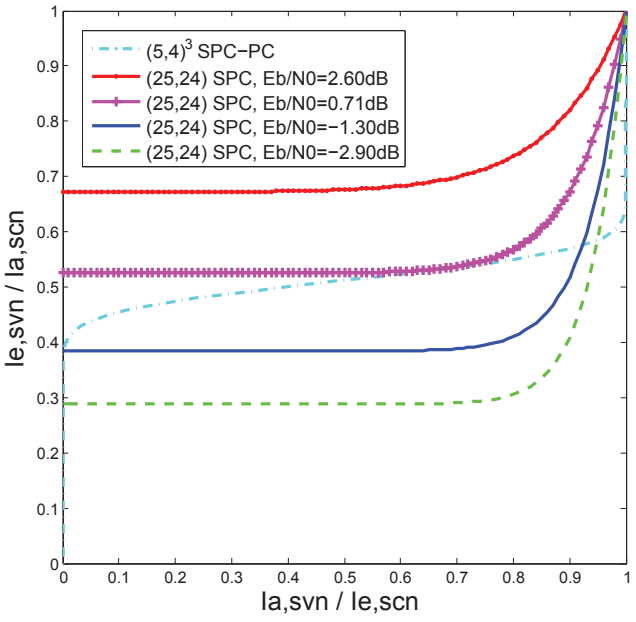

Fig. 7. EXIT chart of a D-GLDPC code with $(25, 24)$ SPC codes as SVNs and $(5, 4)^3$ SPC-PCs as SCNs at different E_b/N_0. The overall code rate is 0.508.

$(25, 24)$ SPC codes as SVNs and $(8, 7)^3$ SPC-PCs as SCNs. The corresponding overall code rate R is 0.656 and the threshold is 1.5 dB, which is only 0.45 dB away from the ultimate Shannon limit.

In Fig. 7, SVNs still use $(25, 24)$ SPC codes, while SCNs use $(5, 4)^3$ SPC-PCs. The overall code rate R is reduced to 0.508. The simulation results show that the threshold is 0.71 dB, only about 0.5 dB away from the ultimate Shannon limit, which is 0.4 dB better than the D-GLDPC code proposed in [12], where R is 0.417 and threshold is about 0.9 dB away from the ultimate Shannon limit.

IV. Conclusion

Motivated by the larger minimum distance of 3-D SPC-PC, we have proposed and analyzed a family of D-GLDPC codes with SPC codes as SVNs and 3-D SPC-PC as SCNs. We have derived the EXIT function of 3-D SPC-PCs used as SCNs. Subsequently, we have used EXIT charts to analyze the decoding threshold and convergence behavior of our proposed D-GLDPC codes. We conclude that D-GLDPC codes with 3-D SPC-PCs as SCNs can offer better performance than using 2-D SPC-PCs in terms of decoding thresholds.

In the future, we plan to investigate efficient and low-complexity D-GLDPC decoding algorithms. We will continue to study the code performance in the waterfall region as well as in the error-floor region. Our aim is to apply the proposed D-GLDPC codes to 5G wireless communication systems.

Acknowledgement

This work was supported in part by the National Natural Science Foundation of China under Grants No. 61372077, No. 60972037 and No. 61372095, the Fundamental Research Program of Shenzhen City under Grants No. JC201005250067A and No. JCJY20120817163755061 and the Technical Research and Development Program of Shenzhen City under Grant No. CXZZ20120615155144842.

The authors would like to thank Y. Min for her significant early work and anonymous reviewers for their helpful comments and suggestions.

References

[1] R. G. Gallager, "Low-density parity-check codes," *IRE Trans. Inform. Theory*, vol. 8, no. 1, pp. 21-28, Jan. 1962.

[2] D. J. C. Mackay and R. M. Neal, "Near Shannon limit performance of low-density parity-check codes," *IEEE Electron. Lett.*, vol. 32, no. 18, pp. 1645-1946, Aug. 1996.

[3] R. M. Tanner, "A recuNrsive approach to low complexity codes," *IEEE Trans. Inform. Theory*, vol. 27, no. 2, pp. 533-547, Sep. 1981.

[4] M. Lentmaier and K. S. Zigangirov, "On generalized low-density parity-check codes based on Hamming component codes," *IEEE Commun. Lett.*, vol. 3, no. 8, pp. 245-250, Aug. 1999.

[5] N. Miladinovic and M. Fossorier, "Generalized LDPC codes with Reed-Solomon and BCH codes as component codes for binary channels," in *Proc. 2005 IEEE Global Telecommunications Conference*, vol. 3, pp. 1239-1244.

[6] I. Djordjevic, L. Xu, T. Wang, and M. Cvijetic, "GLDPC codes with Reed-Muller component codes suitable for optical communications," *IEEE Commun. Letters*, vol. 12, no. 9, pp. 684-686, Sep. 2008.

[7] G. Yue, L. Ping, and X. Wang, "Low-rate generalized low-density parity-check codes with Hadamard contraints," *IEEE Trans. Inform. Theory*, vol. 53, no. 3, pp. 1058-1079, Mar. 2007.

[8] E. Paolono, M. P.C. Fossorier, and M. Chiani, "Generalized and doubly generalized LDPC codes with random component codes for the binary erasure channel," *IEEE Trans. Inform. Theory*, vol. 56, no. 4, pp. 1651-1672, Apr. 2010.

[9] Y. Wang and M. Fossorier, "Doubly generalized LDPC codes," in *Proc. 2006 IEEE International Symposium on Information Theory,* , pp. 669-673.

[10] E.Paolini, M. Chiani and M. Fossorier, "Doubly-generalized LDPC codes: Stability bound over the BEC," *IEEE Trans. Inform. Theory*, vol. 55, no. 3, pp. 1027-1046, Mar. 2009.

[11] E. Paolini, M. F. Flanagan, M. Chiani, and M. Fossorier, "On a class of doubly-generalized LDPC codes with single parity-check variable nodes," in *Proc. 2009 IEEE International Symposium on Information Theory*, pp. 1983-1987.

[12] Y. Min, F. C. M. Lau and C. K. Tse, "Generalized LDPC code with single-parity-check product constraints at super check nodes," in *Proc. 2012 International Symposium on Turbo Codes and Iterative Information Processing*, pp. 165-169.

[13] Y. Min, F. C. M. Lau and C. K. Tse, "A class of doubly-generalized LDPC codes," in *Proc. 2013 International Conference on Advanced Technologies for Communications*, pp. 280-284.

[14] D. Rankin and T. Gulliver, "Single parity check product codes," *IEEE Trans. Commun.*, vol. 49, pp. 1354-1362, Aug. 2001.

[15] S. ten. Brink, G. Kramer, and A. Ashikhmin, "Design of low-density parity-check codes for modulation and detecion," *IEEE Trans. Commun.*, vol. 52, pp. 670-678, Apr. 2004.

[16] A. Ashikhmin, G. Kramer, and S. ten Brink, "Extrinsic information transfer functions: Model and erasure channel properties," *IEEE Trans. Inform. Theory*, vol. 50, no. 4, pp. 2657-2673, Nov. 2004.

[17] E. Sharon, A. Ashikhmin, and S. Litsyn, "EXIT functions for binary input memoryless symmetric channels," *IEEE Trans. Commun.*, vol. 54, no. 7, pp. 1207-1214, July 2006.

[18] Y. Min, F. C. M. Lau and C. K. Tse, "Exact split function for SPC," in *Proc. 2014 International conference on Advanced Technology for Communications*, pp. 1208-1212.